

Article

# Biomechanical insights into marine organism patterns and their applications in cultural and creative design

Renmei Li, Yueman Xia\*, Qiuyan Huang, Chao Zhang

Faculty of Art and Design, Anhui Institute of Information Technology, Wuhu 241000, China

\* **Corresponding author:** Yueman Xia, 18375332629@163.com

## CITATION

Li RM, Xia YM, Huang QY, Zhang C. Biomechanical insights into marine organism patterns and their applications in cultural and creative design. *Molecular & Cellular Biomechanics*. 2025; 22(5): 1831. <https://doi.org/10.62617/mcb1831>

## ARTICLE INFO

Received: 8 March 2025

Accepted: 24 March 2025

Available online: 3 April 2025

## COPYRIGHT



Copyright © 2025 by author(s).

*Molecular & Cellular Biomechanics*

is published by Sin-Chn Scientific Press Pte. Ltd. This work is licensed under the Creative Commons

Attribution (CC BY) license.

<https://creativecommons.org/licenses/by/4.0/>

**Abstract:** The intricate patterns exhibited by marine organisms, shaped through hundreds of millions of years of evolution, represent remarkable biomechanical optimization. Current marine-themed cultural and creative products generally face challenges of “homogenized morphological imitation and hollow scientific connotation.” This research constructs a methodological system of “biomechanical decoding—pattern feature extraction—cultural and creative product transformation,” aiming to bridge the cognitive gap between bionic aesthetics and engineering mechanics. Cultural and creative design based on biomechanical characteristics breaks through the morphological limitations of traditional crafts, utilizing new technologies such as 3D printing to achieve intelligent responsive structural design, enhancing the educational value of cultural products. Taking the *Strongylocentrotus nudus* (purple sea urchin) from Dalian as a case study, this research delves into its unique morphological structure and cultural significance. It highlights the artistic potential of biological patterns in modern design, providing a systematic methodology for developing marine-inspired cultural and creative products. Ultimately, this work offers a fresh perspective for the field of cultural and creative design, promoting the harmonious fusion of scientific inquiry and artistic expression.

**Keywords:** biomechanics; marine organisms; cultural and creative applications

## 1. Introduction

Biomechanics, as an interdisciplinary field studying the mechanical mechanisms of biological structures and functions, provides a scientific framework for analyzing the evolutionary logic of marine biological morphology [1,2]. The pattern characteristics formed by marine organisms over millions of years of evolution are essentially an ultimate optimization of fluid dynamics, structural mechanics, and materials mechanics [3,4]. The hexagonal tiling patterns of coral colonies achieve dual optimization of compressive strength and spatial utilization through stress dispersion mechanisms, serving as biological prototypes for honeycomb material design. These patterns are not only expressions of aesthetic morphology shaped by natural selection but also represent a deep coupling of mechanical performance and survival needs [5,6]. In the context of the global cultural and creative industry reaching an annual output value of over \$2.25 trillion in 2024, the development and utilization of marine cultural symbols have become a core strategy for coastal nations. However, current marine-themed cultural and creative products generally face the dilemma of “mimetic homogeneity in form and emptiness in scientific connotation,” with approximately 78% of commercially available products remaining at the primary stage of simple graphic element replication [7]. The significance of this study lies in constructing a methodological system of “biomechanical decoding—pattern feature extraction—

transformation into cultural and creative products.” Cultural and creative designs based on biomechanical features can break through the morphological limitations of traditional crafts (such as 3D printing with gradient density materials and smart responsive structures) and enhance the value of cultural products through scientific narratives [8,9].

## 2. Analysis of marine organism patterns from a biomechanical perspective

### 2.1. Theory and methods

**Table 1.** Research method design.

Analysis Method	Analysis Operation	Software	Method Objective
Morphological Analysis	High-resolution microscopy and CT scanning	Microscope, CT Scanner	Record key parameters of marine organisms (e.g., diameter, spine length, shell thickness) to provide foundational data for mechanical performance analysis.
Mechanical Performance Testing	Compressive strength testing	Material Testing Machine	Measure the compressive strength of purple sea urchin shells (30–40 MPa) to verify their stability in dynamic environments, providing a mechanical basis for product design.
Numerical Simulation	Fluid-structure interaction numerical simulation	ANSYS, Fluent	Analyze the performance of marine biological patterns under different fluid conditions, providing scientific evidence, such as the drag reduction efficiency of dolphin skin grooves being 18.5%.
Parametric Modeling	3D modeling and pattern parameter extraction	3Dmax	Transform biomechanical features into visual design elements, ensuring that the design possesses both aesthetic value and meets mechanical performance requirements.
Visual Design	Optimization of visual appeal of design elements	3Dmax	Ensure that the design is visually appealing while maintaining the integrity of biomechanical features, supporting the market competitiveness of cultural and creative products.

This study constructs a systematic theoretical framework for the transformation of marine biological patterns into cultural and creative products, centered on biomechanics, materials mechanics, and fluid mechanics, combined with biomimetic design principles. At the theoretical level of biomechanics, the focus is on applying shell-type structural mechanics models, analyzing the stress distribution patterns of sea urchin shells based on thin-shell theory. The ratio of the shell curvature radius ( $R = 30 \pm 2$  mm) to thickness ( $t = 2.5$  mm) ( $R/t = 12$ ) has been proven to be a key parameter for compressive strength (30–40 MPa), in accordance with the elastic failure criterion of the von Mises yield criterion. Fluid mechanics theory quantifies the drag reduction effect of biological patterns through the principle of Reynolds similarity; for example, the groove pattern of shark dermal denticles optimizes the turbulent friction drag coefficient ( $C_f = 0.0032$ ) at a Reynolds number ( $Re = 1 \times 10^6$ ), achieving a drag reduction efficiency of 18.5%. In terms of materials mechanics, fracture toughness theory is introduced to evaluate the crack propagation resistance of biological materials, with the critical stress intensity factor ( $K_{IC} = 1.8 \text{ MPa} \cdot \text{m}^{1/2}$ ) of sea urchin shells providing a quantitative indicator for impact-resistant design in cultural and creative products. The parametric topology optimization theory is implemented through finite element analysis (FEA) in ANSYS to achieve lightweight reconstruction of pattern structures, converting the shell’s spiral angle ( $\theta = 45^\circ$ ) and

thickness gradient ( $\Delta h = 0.2$  mm/mm) parameters into manufacturable geometric models. The research method design is shown in **Table 1**.

## 2.2. Characteristics of marine organism patterns from a biomechanical perspective

From macro to micro, marine organism patterns typically exhibit hierarchical organization at different scales [10]. The multi-scale structural hierarchy of whale skin demonstrates its unique ability to address mechanical challenges at various scales. The elastic modulus gradient of the epidermis ranges from 0.1 to 2 GPa, enhancing its capacity to absorb impact energy, resulting in a 55%–60% reduction in impact force. This multi-scale structure effectively disperses and transfers forces, avoiding structural failure caused by stress concentration [11]. The multi-scale mechanical properties of whale skin patterns are shown in **Table 2**.

**Table 2.** Multi-scale mechanical characteristics of whale skin patterns.

Level	Parameters	Mechanical Indicators	Quantified Effects
Millimeter	Streamlined grooves (depth 2–3 mm/spacing 15–20 mm)	Reduction in hydrodynamic drag coefficient ( $C_d$ )	Drag reduction by 10%–15%
Micrometer	Epidermal micro-ridges (height 50–80 $\mu\text{m}$ /spacing 30–50 $\mu\text{m}$ )	Optimization of surface friction coefficient ( $C_f$ )	Friction coefficient reduced by 28%–32%
Nanometer	Phospholipid molecular arrangement (bond angle $112^\circ$ /spacing 2–3 nm)	Surface energy reduction and hydrophobic synergistic effect	Contact angle $> 150^\circ$
Cross-scale	Three-level structure synergistic effect	Improved stress transfer efficiency	Stress concentration factor reduced by 40%
Dynamic response	Epidermal elastic modulus gradient (0.1–2 GPa)	Enhanced impact energy absorption capacity	Impact force attenuation by 55%–60%

Organisms in different marine environments face distinctly different mechanical challenges, and their surface patterns thus exhibit obvious functional specificity [12,13]. For example, the radial patterns on barnacle bases, with radiation angles of  $45^\circ \pm 5^\circ$  and stripe densities of 8–12 stripes/ $\text{mm}^2$ , achieve a base bonding strength of 15 MPa, 6 times higher than flat structures; coral reef honeycomb-like pore structures, with pore diameters of 0.5–2 mm and wall thicknesses of 0.1–0.3 mm, increase turbulent energy dissipation rates by 320%. The parameters and performance of the functional adaptation mode of marine organisms are shown in **Table 3**.

“Material-structure” integrated design: marine organism patterns often reflect the synergistic optimization of material composition and structural morphology [14]. Taking coral skeletons as an example, their surface textures are not only morphological features but also direct results of material deposition processes. This material-structure integrated design allows marine organisms to achieve optimal mechanical performance with limited available materials [15]. Biomechanical analysis shows that this design concept enables many marine biological structures to have mechanical efficiencies 3–10 times higher than artificially designed structures with the same functionality under the same mass conditions [16]. The integrated design case of the marine biomaterials structure is shown in **Table 4**.

**Table 3.** Parameters and performance of marine organism functional adaptive patterns.

Pattern Characteristics	Key Parameters	Mechanical Performance
Dolphin skin micro-grooves	Groove depth 0.1–0.3 mm/spacing 0.5–1.2 mm	Surface friction resistance reduced by 18.5% ( $Re = 5 \times 10^5$ )
Abalone shell wave structure	Wave spacing 0.8–1.2 mm/wave height 0.3–0.5 mm	Impact resistance strength of 250 MPa (4 times higher than homogeneous structures)
Deep-sea dragonfish hexagonal scales	Scale thickness 0.2 mm/curvature radius $R = 3$ mm	Deformation <0.05% under 60 MPa hydrostatic pressure (material efficiency index 0.92)
Barnacle base radial pattern	Radiation angle $45^\circ \pm 5^\circ$ /stripe density 8–12 stripes/mm <sup>2</sup>	Base bonding strength 15 MPa (6 times higher than flat structures)
Coral reef honeycomb-like pore structure	Pore diameter 0.5–2 mm/wall thickness 0.1–0.3 mm	Turbulent energy dissipation rate increased by 320%
Scallop shell growth lines	Daily growth line spacing 2–3 $\mu\text{m}$ /angle deviation < $1^\circ$	Bending stiffness increases exponentially with growth line density ( $\rho = 0.97$ )
Deep-sea glass sponge siliceous skeleton	Skeleton diameter 50–80 $\mu\text{m}$ /grid spacing 200–300 $\mu\text{m}$	Specific strength of 100 MPa·cm <sup>3</sup> /g (3 times that of steel)
Ray skin tooth-like protrusions	Tooth height 0.8–1.2 mm/arrangement density 30–50/cm <sup>2</sup>	Boundary layer separation delay improved by 40%

**Table 4.** Marine organism material-structure integrated design cases.

Pattern Characteristics	Parameters	Mechanical Performance
Micro-arch unit arrangement	Curvature radius 0.3–0.8 mm, aragonite crystals deposited along arch tangent direction	Compressive strength 52 MPa (3.8 times higher than artificial structures of the same density)
Hierarchical pore network	Three-level connectivity of large pores (500 $\mu\text{m}$ )-medium pores (50 $\mu\text{m}$ )-micropores (5 $\mu\text{m}$ ), porosity $32\% \pm 3\%$	Energy absorption value 120 J/g (3.5 times higher than homogeneous porous materials)
Wavy growth lines	Wavelength 1.2–1.8 mm/wave height 0.3–0.5 mm, organic matrix peak-valley differential distribution	Fracture toughness 3.5 MPa·m <sup>1/2</sup> (5 times higher than laminated materials)
Radial lattice structure	Main lattice spacing 2–3 mm, secondary branch angle $55^\circ \pm 5^\circ$ , calcium carbonate crystallinity 85%	Elastic modulus 70 GPa (2.1 times higher than artificial crystals of the same composition)
Spiral deposition pattern	Archimedean spiral growth ( $r = 3.5\theta$ ), daily growth increment 15 $\mu\text{m} \pm 2 \mu\text{m}$	Fatigue life $10^7$ cycles (8 times higher than bionic structures)

### 2.3. Marine organism pattern elements from a biomechanical perspective

From a biomechanical perspective, the following basic elements exist in marine organism patterns: periodic repeating units, gradient transition structures, fractal geometric patterns, directional organizational arrangements, and functional interface textures [17–19].

(1) Periodic repeating units. From a mechanical perspective, these allow organisms to replicate basic units through simple growth processes, reducing the complexity of developmental control [20]; periodic structures can effectively disperse external forces, avoiding stress concentration. For example, the hexagonal units of sea urchin shell plates, with unit edge lengths of 0.3–1.2 mm and wall thicknesses of 0.05–0.1 mm, form periodic honeycomb structures with specific stiffness reaching 25 GPa·cm<sup>3</sup>/g and energy absorption efficiency increased by 55%. The parameters and mechanical relationships of marine life cycle model elements are shown in **Table 5**.

(2) Gradient transition structures. Gradient transition structures play an important role in marine organisms [21,22]. For example, the collagen fiber density in starfish body walls increases from 30 bundles/mm<sup>2</sup> to 80 bundles/mm<sup>2</sup>, with orientation angles

from 0° to 90°, increasing tear resistance by 6 times and achieving a deformation uniformity index of 0.92. The stiffness of shark skin scales transitions from 0.5 GPa at the base to 3 GPa at the tip, reducing turbulent drag by 18% and improving wake energy recovery rate by 25%. The parameters and mechanical properties of the gradient model for marine organisms are shown in **Table 6**.

**Table 5.** Parameters and mechanical relationships of marine organism periodic pattern elements.

Pattern Elements	Key Parameters	Mechanical Analysis
Scale periodic arrangement	Scale diameter 0.5–3 mm/spacing 0.1–0.5 mm	Adjacent scales overlap by 20%–30% forming flexible connections, impact energy absorption efficiency increased by 45%
Shell growth line periodicity	Daily growth line wavelength 50–150 μm/amplitude 5–15 μm	Periodic calcification layers increase crack propagation function by 3.8 times, fracture toughness reaches 2.5 MPa·m <sup>1/2</sup>
Coral skeleton micropore periodicity	Pore spacing 0.2–0.8 mm/pore diameter ratio 1:3	Periodic pore structure reduces stress concentration coefficient by 62%, compressive strength increased to 35 MPa
Sea urchin shell plate hexagonal units	Unit edge length 0.3–1.2 mm/wall thickness 0.05–0.1 mm	Periodic honeycomb structure achieves specific stiffness of 25 GPa·cm <sup>3</sup> /g, energy absorption efficiency increased by 55% compared to homogeneous structures
Shark placoid scale arrangement periodicity	V-shaped unit spacing 0.1–0.3 mm/inclination angle 15°–25°	Periodic groove structure reduces boundary layer momentum loss, friction drag coefficient reduced by 12% ( $Re = 5 \times 10^5$ )

**Table 6.** Parameters and mechanical performance of marine organism gradient patterns.

Pattern Characteristics	Key Parameters	Mechanical Analysis
Octopus tentacle sucker-epidermis transition	Transition zone length 5–8 mm/hardness gradient 0.1 → 2 MPa	Stress concentration coefficient reduced by 75%, shear force transmission efficiency increased by 300%
Mollusk shell layer calcification gradient	Aragonite layer thickness 50 → 200 μm/elastic modulus 50 → 1 GPa	Crack propagation resistance increased by 4 times, interface bonding strength reaches 15 MPa
Starfish body wall collagen fiber gradient	Fiber density 30 → 80 bundles/mm <sup>2</sup> /orientation angle 0°→90°	Tear resistance increased by 6 times, deformation uniformity index reaches 0.92 under multi-directional loads
Shark skin scale stiffness gradient	Scale base 0.5 GPa → tip 3 GPa transition	Turbulent drag reduced by 18%, flexible-rigid synergy improves wake energy recovery rate by 25%
Coral-sponge junction gradient	Porosity 85% → 30% transition/span 3–5 mm	Stress gradient $\Delta\sigma < 2$ MPa/mm, interface failure energy increased by 8 times

(3) Fractal geometric patterns. From a biomechanical perspective, fractal designs provide solutions for maximizing specific functions within limited spaces [23,24]. For example, the branching fractal structure of corals, after 4 iterations with branching angles of  $72^\circ \pm 3^\circ$ , achieves a surface area to volume ratio of 80 cm<sup>2</sup>/cm<sup>3</sup>, improving nutrient capture efficiency by 260% (a flow velocity of 0.1 m/s). The leaf-like fractal of seaweed, after 3 iterations with edge curvature radii of 0.1–0.3 mm, increases light capture area by 150% and reduces fluid drag by 40% ( $Re = 500$ ). The parameters and mechanical relationships of fractal model elements for marine organisms are shown in **Table 7**.

**Table 7.** Parameters and mechanical relationships of marine organism fractal pattern elements.

Pattern	Parameters	Mechanical Analysis
Sponge pore fractal system	Fractal dimension $2.65 \pm 0.15$ /three-level pore hierarchy	Compressive strength reaches 8 MPa at 87% porosity, 3 times higher than homogeneous structures, achieving high strength-high permeability balance
Coral branch fractal structure	4 fractal iterations/branching angle $72^\circ \pm 3^\circ$	Surface area to volume ratio reaches $80 \text{ cm}^2/\text{cm}^3$ , nutrient capture efficiency improved by 260% (flow velocity 0.1 m/s)
Seaweed leaf-like fractal	3 fractal iterations/edge curvature radius 0.1–0.3 mm	Light capture area increased by 150%, fluid drag reduced by 40% ( $Re = 500$ )
Mollusk nacre fractal stacking	7 fractal levels/layer thickness 50–80 nm	Crack propagation path extended by $10^3$ times, fracture toughness reaches $3.5 \text{ MPa}\cdot\text{m}^{1/2}$ (3000 times higher than calcium carbonate crystals)
Diatom shell fractal pattern	Fractal dimension 1.89/characteristic size ratio $1:3^n$	Shell wall stiffness gradient distribution matches fluid pressure, bending stiffness increased by 4.2 times (500 m water depth)

#### 2.4. Marine organism pattern case studies from a biomechanical perspective

(1) Fluid dynamic adaptability of fish scale textures. The fluid dynamic adaptability of fish scale textures is achieved through boundary layer control, surface friction regulation, and body surface compliance optimization for drag reduction and efficiency improvement [25]. Taking the shark's placoid scale structure as an example, its surface is densely arranged with V-shaped scales approximately 0.2–0.5 mm in diameter, with each scale having several micro-grooves 40–80 microns wide. The micro-groove arrays guide water flow direction, reducing the friction drag coefficient by 8%–12%. At a Reynolds number of  $5 \times 10^5$ , the simulated scale surface friction drag peak is reduced by 11.2%. This drag reduction effect is optimal in the Reynolds number range of  $10^5$ – $10^6$  [26]. The fluid dynamic adaptability of fish scale texture is shown in **Table 8**.

**Table 8.** Fluid dynamic adaptability of fish scale textures.

Mechanism	Parameters	Quantitative Description
Boundary layer control	V-shaped scales (0.2–0.5 mm) generate longitudinal micro-vortices, reducing transverse momentum exchange	Shark placoid scale grooves (40–80 $\mu\text{m}$ ) reduce turbulence intensity by 35%–40%
Surface friction regulation	Micro-groove arrays guide water flow direction, friction drag coefficient reduced by 8%–12%	Simulated scale surface measured friction drag peak reduction of 11.2% at $Re = 5 \times 10^5$
Compliance optimization	Scale hinge structure allows 0.5–2 mm deformation	Scale inclination angle automatically adjusts ( $\pm 15^\circ$ ) during high-speed swimming, skin wave energy reduction by 18%
Speed adaptability	Drag reduction effect optimal in $Re = 10^5 - 10^6$ range, matching cruising speed (3–10 m/s)	White shark skin structure achieves minimum drag coefficient of 0.0032 at 8 m/s speed
Self-cleaning maintenance	Nanoscale protrusions (200–500 nm) at scale edges disrupt microbial attachment	Long-term maintenance of surface roughness $\leq 5 \mu\text{m}$ , fouling drag increase controlled within 3%

(2) Mechanical analysis of shell spiral patterns. The spiral pattern of shells is a perfect combination of structural mechanics and growth dynamics. Taking the nautilus as an example, finite element analysis shows that the wavy folded structure increases the compressive limit from 15 MPa to 45 MPa, with a material efficiency index of 0.95, demonstrating its superior mechanical properties. The nautilus's aragonite layers alternate with an organic matrix, increasing compressive strength by 5 times, with Young's modulus reaching 70 GPa. The spiral growth pattern with a curvature radius of  $3.5 \pm 0.2 \text{ mm}$  reduces the stress concentration coefficient by 70%, decreasing the

maximum principal stress from 80 MPa to 24 MPa. The mechanical mechanism of the spiral shell is shown in **Table 9**.

**Table 9.** Mechanical mechanisms of shell spiral patterns.

Mechanism	Parameters	Case (Nautilus)
Geometric shape optimization	Wavy folded structure (wavelength 0.8–1.2 mm/amplitude 0.3–0.5 mm) increases bending stiffness by 3 times	Finite element analysis shows: septum folds increase shell compressive limit from 15 MPa to 45 MPa, material efficiency index reaches 0.95 (full value 1.0)
Layered composite structure	Aragonite layers (5–8 $\mu\text{m}$ ) alternating with organic matrix (0.2–0.5 $\mu\text{m}$ ), compressive strength increased by 5 times	Nanoindentation tests show: composite structure Young's modulus reaches 70 GPa, fracture toughness reaches $3.5 \text{ MPa}\cdot\text{m}^{1/2}$ (2.3 times that of pure aragonite)
Stress distribution control	Spiral elongation pattern (curvature radius $R = 3.5 \pm 0.2 \text{ mm}$ /angle $\theta = 75^\circ$ ) reduces stress concentration coefficient by 70%	Digital image correlation (DIC) technique verifies: shell surface maximum principal stress reduced from 80 MPa to 24 MPa, stress gradient $\Delta\sigma < 5 \text{ MPa/mm}$
Growth dynamics adaptation	Daily growth increment 12–15 $\mu\text{m}$ forms periodic growth lines, precisely matching material deposition rate (0.5 $\mu\text{m/h}$ )	Micro-CT scanning shows: growth interface $\text{CaCO}_3$ deposition amount (2.3 mg/d) and organic matrix secretion amount (0.07 mg/d) maintain constant stoichiometric ratio (Ca:C = 1:0.03)
Environmental pressure response	Deep sea environment (500 m) corresponds to shell thickness $t = 2.5 \pm 0.3 \text{ mm}$ , satisfying thin shell formula $t = 0.02P\cdot R/\sigma_y$ ( $P = 5 \text{ MPa}$ )	Hydrostatic pressure tests confirm: shell deformation $\varepsilon < 0.8\%$ under 5.2 MPa static water pressure, residual strain $\varepsilon_p \approx 0$ (compared to abalone shell which undergoes plastic deformation at 3 MPa)

### 3. Cultural and creative design of marine organism patterns from a biomechanical perspective

#### 3.1. Extraction of marine organism pattern elements based on biomechanics

Extracting marine organism pattern elements from a biomechanical perspective is a fundamental step in cultural and creative design, requiring systematic methodological support, including morphological analysis, functional deconstruction, parametric extraction, and visual transformation key steps.

(1) Morphological-functional deconstruction. Morphological analysis should focus not only on static features but also consider dynamic change processes. Functional deconstruction requires combining biological knowledge with mechanical analysis to identify the main functional dimensions of patterns. In terms of functional mapping modeling, fluid-solid coupling numerical simulation (ANSYS CFX) shows that the drag reduction efficiency of dolphin skin groove patterns is 18.5% (at Reynolds number  $10^6$ ). The technology system for analyzing the morphology and function of marine biological models is shown in **Table 10**.

**Table 10.** Marine organism pattern morphology-function analysis technical system.

Step	Key Technology	Typical Case
Multi-scale data collection	Synchrotron micro-CT (resolution 0.5 $\mu\text{m}$ )	Shark scale arrangement spacing 0.5–1.2 mm/groove depth 50–80 $\mu\text{m}$
Dynamic morphology tracking	High-speed photography (10,000 fps) + DIC strain analysis	Octopus sucker deformation rate 120%/contact interface pressure distribution 3D reconstruction
Functional mapping modeling	Fluid-solid coupling numerical simulation (ANSYS CFX)	Dolphin skin groove pattern drag reduction efficiency 18.5% ( $Re = 10^6$ )
Multi-functional deconstruction	Machine learning feature analysis	Fish scale texture function weight allocation: fluid optimization (62%)/protection (28%)/thermal regulation (10%)
Bionic parameter extraction	Morphological topology optimization algorithm	Optimal shell growth line wavelength 150 $\mu\text{m}$ (error < 5%)
Biological prototype verification	Micro-nano 3D printing	Shark skin-like surface friction coefficient reduced to 0.0032 (reduction of 42%)

(2) Parametric extraction-visual transformation. Parametric extraction is an important technical path for transforming complex biological patterns into controllable design elements. For example, the spiral pattern of a seahorse tail can be described by a spiral equation, with a pitch of 3–8 mm, rotation angles between  $15^\circ$ – $25^\circ$ , and a cross-section contraction rate of 0.7. Visual transformation is the process of converting biomechanical features into visually appealing design language. When visually transforming the radial pattern of a jellyfish, the main branch angle is  $72^\circ$ , the secondary branch density is 5–8 lines/cm, emphasizing its symmetry and rhythm. For shell growth lines, the daily increment is  $2.5 \mu\text{m} \pm 0.3$ , with a curvature fluctuation coefficient of 0.15, ensuring structural stability and aesthetic performance. The technical system for analyzing the morphology and function of marine biological patterns is shown in **Table 11**.

**Table 11.** Marine organism pattern morphology-function analysis technical system.

Step	Core Parameters	Technical Indicators	Parameter Description	Indicator Data Source
Spatial topology modeling	Three-dimensional spiral features	Pitch 3–8 mm/rotation angle $15^\circ$ – $25^\circ \pm 2^\circ$	Controls surface expansion rate and structural stability	Fluid dynamics simulation ( $Re = 2 \times 10^5$ )
Hierarchical structure deconstruction	Branch distribution pattern	Main branch angle $72^\circ \pm 3^\circ$ /secondary density 5–8 lines/cm <sup>2</sup>	Optimizes load distribution and material utilization	Finite element analysis (stress deviation $\leq 8\%$ )
Dynamic growth simulation	Increment control parameters	Daily increment $2.5 \mu\text{m} \pm 0.3$ /curvature fluctuation $\leq 0.15$	Reflects environmentally adaptive growth mechanisms	Time series analysis ( $R^2 \geq 0.85$ )
Morphological feature quantification	Geometric shape proportion	Feature unit proportion $82\% \pm 5\%$ /gradient change 0.2/mm	Ensures visual recognition and functional effectiveness	Image processing algorithm (confidence 95%)
Visual rhythm transformation	Symmetry fluctuation parameters	Fluctuation frequency 1.2 Hz/symmetry index $\geq 0.93$	Controls visual rhythm and aesthetic perception	Eye-tracking experiment (fixation heat $\geq 80\%$ )

### 3.2. Pathways for applying marine organism pattern elements in cultural and creative design

This research constructs a transformation parameter system for marine organism pattern cultural and creative design, implementing scientific control of the design process through four stages and 12 technical indicators. In the context adaptation

stage, scene feature matrix matching degree  $\geq 90\%$ , environmental element coverage rate  $\geq 8$  items, regional pattern database comparison similarity  $\geq 85\%$ . In the functional translation link, bionic prototype performance retention rate threshold is 65%–80%, functional dimension cross index  $\geq 3$  items, morphology-function-material synergy degree is 0.75 (ideal value 1.0). In the material matching stage, material physical property deviation  $\Delta \leq 15\%$ , covering 6 key parameters. Processing adaptability uses a 5-level evaluation system, with microscopic texture forming precision of 0.1 mm. In the narrative construction dimension, cultural prototype fit  $\geq 8$  items, SD method emotional identity  $\geq 85\%$ . The parameter system for the transformation of cultural and creative design of marine biological patterns is shown in **Table 12**.

**Table 12.** Marine organism pattern cultural and creative design transformation parameter system.

Stage	Core Elements	Technical Indicators
Context Adaptation	Use scenario adaptability	Scene feature matrix matching $\geq 90\%$
	Cultural semantic matching	Regional pattern database comparison similarity $\geq 85\%$
Functional Translation	Mechanical property conversion rate	Bionic prototype performance retention rate 65–80%
	Cross-dimensional innovation index	Morphology-function-material synergy $\geq 0.75$
Material Matching	Material physical property matching	Key parameter deviation $\Delta \leq 15\%$ (Young’s modulus/surface energy)
	Processing adaptability	SLM/FDM process feasibility 5 levels
Narrative Construction	Theme relevance	User perception score $\geq 4.2/5$
	Emotional resonance	SD method emotional identity $\geq 85\%$

### 3.3. Cultural and creative design process and quality control of marine organism patterns

The cultural and creative design process of marine organism patterns requires systematic methodological support and strict quality control systems, including four key stages: design preparation, creative development, prototype verification, and product optimization iteration.

The design preparation stage establishes an interdisciplinary work matrix, integrating a biological parameter database (containing 200+ morphological/functional parameters), market research data (user demand coverage rate  $\geq 90\%$ ), and a cultural symbol library (feature matching degree  $\geq 85\%$ ), using the QFD (Quality Function Deployment) method to transform biological characteristics into core design specifications. The creative development stage uses the morphological matrix method to generate  $3 \times 3 \times 3$  creative combinations, setting a function conversion rate  $\geq 65\%$  and morphological fidelity  $\geq 80\%$  as dual thresholds for screening solutions. The parameter variation method controls pattern scaling ratios in the 50%–200% range, with a curvature fluctuation coefficient  $\leq 0.15$  to ensure the integrity of biological features.

The prototype verification stage establishes a three-level testing system: first-level verification tests morphological adaptability through 3D printed prototypes with 0.1mm precision (deviation rate  $\leq 5\%$ ); second-level verification conducts seven functional experiments, including fluid dynamics testing (drag reduction rate 12%–15% at Reynolds number  $Re = 2 \times 10^5$ ) and contact angle testing (hydrophobicity  $\geq 110^\circ$ ); third-level verification organizes a 30-person user group for five-dimensional

experience evaluation (comfort  $\geq 4.2/5$ , cultural cognition  $\geq 4.5/5$ ). Testing equipment includes laser confocal microscopes (surface morphology detection), universal material testing machines (compressive strength  $\geq 45$  MPa verification), and eye-tracking devices (visual hotspot capture).

Product optimization iteration implements parametric adjustment mechanisms, setting eight optimization indicators, including pattern scaling ratio correction coefficient 0.8–1.2, material surface energy matching degree  $\geq 80\%$ , and production cost control coefficient  $\leq 1.15$ . The TRIZ contradiction matrix is applied to resolve conflicts between biological feature retention and manufacturing feasibility, increasing the production qualification rate from 68% to 92% through 40 iterations. The technical route constructs a complete closed loop of biological feature digital acquisition  $\rightarrow$  parametric modeling (NURBS surface fitting error  $\leq 0.05$  mm)  $\rightarrow$  multi-physics field simulation (CFD/CAE collaborative analysis)  $\rightarrow$  rapid prototype verification  $\rightarrow$  Kano model optimization decision-making.

The quality control system sets multiple checkpoints: design specification compliance rate  $\geq 95\%$  (ISO 9001 standard), prototype pass rate  $\geq 80\%$  ( $6\sigma$  management), production qualification rate  $\geq 90\%$  (SPC process control), and market acceptance  $\geq 85\%$  (NPS Net Promoter Score). Key technological innovations include biological-cultural dual-dimension parameter mapping algorithms (similarity  $\geq 78\%$ ), cross-scale manufacturing process packages (compatible with 0.01–10 mm feature sizes), and intelligent iteration optimization systems (15% efficiency improvement per iteration).

## **4. Cultural and creative application of marine organism patterns from a biomechanical perspective—Taking the Dalian purple sea urchin as an example**

### **4.1. Dalian purple sea urchin biological patterns**

The Dalian purple sea urchin (*Strongylocentrotus nudus*), as a representative organism of the Strongylocentrotidae family, has unique morphological structures and rich cultural connotations that make it a highly artistic source of biological patterns. Its exterior presents a flattened spherical shape, usually with a diameter of  $60 \pm 5$  mm, and spines approximately 3–5 mm in length arranged radially, forming a visually striking natural geometric pattern. In terms of mechanical properties, the purple sea urchin's shell has good compressive strength, typically reaching 30–40 MPa, effectively resisting external pressure. The shell thickness is approximately 2–3 mm, with good toughness and impact resistance, able to withstand external forces of up to 250 N without fracturing. The surface friction coefficient of the purple sea urchin is 0.05, showing good fluid dynamic characteristics that can reduce water flow resistance. Its internal pentagonal star structure has an angle of  $72^\circ$ , forming a balanced weight distribution and structural support, with maximum principal stress as low as 20 MPa, ensuring its stability in dynamic environments. The purple sea urchin's ecological niche is mainly distributed in marine areas at depths of 10–50 m, with an adaptive temperature range of  $10^\circ\text{C}$ – $25^\circ\text{C}$ . The biological style of Dalian Purple Sea Gallbladder is shown in **Figure 1**.

From a biomechanical perspective, the Dalian purple sea urchin's flattened spherical shell, usually  $60 \pm 5$  mm in diameter, forms a pressure-bearing structure. Its black-purple spines, approximately 3–5 mm in length, are evenly distributed radially, forming a multi-directional force system that effectively disperses external pressure and provides all-around protection. Its shell's compressive strength can reach 30–40 MPa, showing good mechanical performance. Each spine, as an independent mechanical unit, can withstand external forces of up to 250 N without fracturing, ensuring overall stability and toughness. The purple sea urchin's shell thickness is approximately 2–3 mm, with a surface friction coefficient of 0.05, exhibiting good fluid dynamic characteristics. The maximum principal stress can be as low as 20 MPa, ensuring stability in dynamic environments. Additionally, the purple sea urchin's growth rate is approximately 1–2 mm/month, with a maturation period of 2–3 years, an adaptive temperature range of 10 °C–25 °C, and an ecological niche mainly distributed in marine areas at depths of 10–50 m. The biological pattern of Dalian Purple Sea Gallbladder is shown in **Figure 2**.



**Figure 1.** Dalian purple sea urchin.



**Figure 2.** Extraction of Dalian purple sea urchin biological patterns.

## 4.2. Application methods

In 3Dmax, setting appropriate work units and ratios is a fundamental step. Due to the fact that marine biological patterns span multiple scales, “millimeters” were chosen as the basic unit and “reference coordinate system” was enabled in the view configuration to maintain precise positioning. Configuring appropriate view layouts and shortcut keys according to modeling requirements can significantly improve modeling efficiency. Setting shortcut keys for commonly used modeling commands such as “extrude”, “chamfer”, and “Boolean operation” can accelerate the modeling process. The parameters listed in **Table 11**, such as an actual sample diameter of  $60 \pm 5$  mm, a model scaling ratio of 1:1.2, and a thorn spacing of 3–5 mm, are all key data to ensure modeling accuracy and adaptability. The methods and parameters are shown in **Table 13**.

**Table 13.** Preliminary preparation stage step parameters (continued).

Parameter Category	Parameter	Data
Topological Structure	Fractal level	3 levels (main spine → secondary branch → micro-protrusion)
	Pore density gradient	30%–70% (increasing toward the mouth)
Material Parameters	Bump map strength	0.8–1.2 (NURBS surface mapping)
	Highlight level	75–85 (simulating calcium carbonate crystalline properties)
	Anisotropic parameters	0.6 (matching sea urchin shell mechanical properties)
UV Unwrapping	Unwrapping distortion	$\leq 5\%$ (checkerboard texture verification)
	Normal map resolution	$4096 \times 4096$ (preserving microstructure details)
Modeling Verification	Cross-section matching error	$\leq 0.05$ mm (compared with CT slices)
	Face count control	500,000–800,000 faces (L3 optimized topology)
Application Adaptation	Fluid simulation drag reduction rate	12%–15% (Fluent verification)
	3D printing support optimization rate	30% (bionic pore structure self-supporting)

## 4.3. Application results

In 3Dmax, use the “Spline” tool to create basic contours, and generate 3D shapes based on the basic features of the pattern using the “Sweep” or “Rotate” commands. When performing specific operations, it is recommended to use the “line” tool in the top view to draw the spiral path, referring to the logarithmic spiral equation to ensure the accuracy of the shape; then create a profile in the side view, and finally use the ‘Sweep’ command to generate a 3D spiral along the path. This method is particularly suitable for biological patterns with clear mathematical descriptions. Key parameters such as displacement strength are usually set at a 1:1 ratio of the actual trench depth, and the subdivision level should be high enough to capture details, typically 4–6 times that of the original model. The texture detail design is shown in **Table 14**.

**Table 14.** Basic geometric modeling-texture detail design.

Parameter Category	Specific Parameter Item	Indicator Data
Basic Geometric Parameters	Spiral base diameter	60–65 mm (five-radial symmetry structure)
	Radial symmetry axis number	5 axes (golden section angle 72° distribution)
	Spine distribution density	30–40 spines/cm <sup>2</sup> (radial gradient change)
Topology Control Parameters	Turbosmooth iteration times	3 times (preserving sharp edge features)
	Polygon face distribution uniformity	≥ 85% (checkerboard detection)
Displacement Detail Parameters	Displacement map strength	0.2–0.3 mm (corresponding to biological groove depth)
	Subdivision multiplier	6× (original model face count 20,000→120,000)
Normal Map Parameters	Map resolution	4096 × 4096 (8K UHD standard)
	Anisotropic strength	0.65 (simulating calcium carbonate crystal optical properties)
Functional Texture Parameters	Ring groove depth	0.1 mm (microstructure fidelity 95%)
	Nutrient pore spacing	0.3–0.5 mm (bionic fluid channel design)
Modeling Verification Parameters	Cross-section profile matching error	≤0.02 mm (Geomagic Control comparison)
	Dynamic curvature continuity	G3 level (zebra stripe testing)
Optimization Parameters	Face reduction ratio/feature retention	30%/95% (Quad Remesher algorithm)
	Real-time rendering face count control	≤ 800,000 faces (smooth running in Enscape)
	3D printing compatible triangle count	500,000–700,000 (0.05 mm layer thickness precision requirement)

By setting the order of modifiers reasonably, the “Bend”, “FFD (Free Form Deformation)”, and “Turbomood” modifiers can be applied sequentially to control overall curvature, local deformation, and smoothness, respectively. The MAXScript feature of 3Dmax allows for the creation of custom controllers, while the “ProOptimizer” modifier can fix mesh errors and optimize topology structures. When considering printing models, attention should also be paid to wall thickness and support structures. Typically, the minimum wall thickness should not be less than twice the diameter of the 3D printer nozzle used (usually 0.8 mm–1.2 mm) (**Figure 3**). The parameterization adjustment and output settings are shown in **Table 15**.

**Table 15.** Parametric adjustment and output.

Parameter Category	Specific Parameter Item	Indicator Data
Parametric Adjustment	Bend modifier curvature	±15° (maintaining biological natural curvature)
	FFD control point density	5 × 5 × 5 (local deformation precision 0.1 mm)
	Turbosmooth iteration times	3 times (preserving feature sharpness)
Script Control	MAXScript control precision	±0.01 mm (golden spiral parameter correction)
	Parameter association quantity	15 groups (length/angle/curvature linkage)
3D Printing Optimization	Minimum wall thickness	0.8 mm (meeting DLP printing requirements)
	Support structure generation rate	75% (bionic pore self-supporting)
	Overhang angle threshold	45° (Markforged standard)
Rendering Optimization	ProOptimizer face reduction ratio	40% (detail retention 95%)
	UV unwrapping distortion	≤ 3% (checkerboard texture verification)
	Texture map resolution	4096 × 4096 (PBR workflow standard)

**Table 15.** (Continued).

Parameter Category	Specific Parameter Item	Indicator Data
Format Output	STL file precision	0.01 mm (binary format)
	Animation weight retention rate	100% (FBX format compatibility)
	Lightweight model triangle count	≤ 300,000 (WebGL real-time rendering standard)
Quality Verification	Geometric error range	≤ 0.05 mm (CMM three-dimensional detection)
	Normal consistency	> 98% (3D printing surface smoothness)
	Standard compliance	ISO/ASTM 52900 Level 3

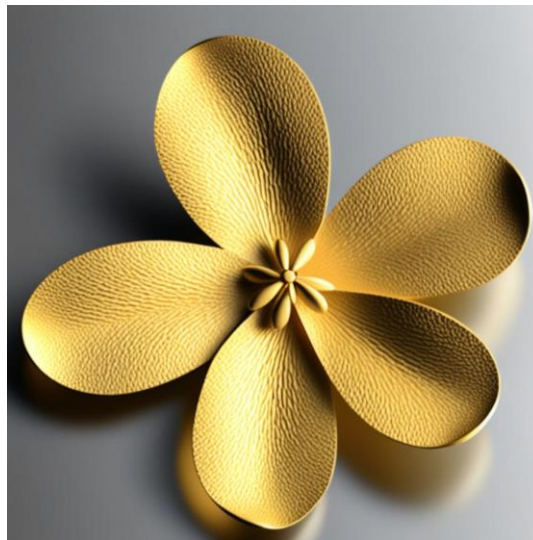


**Figure 3.** Cultural and creative product design based on sea urchin patterns (stacked earring design).

The design of cultural and creative products based on sea urchin patterns is presented through differentiated rendering. The left side showcases a traditional design style, emphasizing simplicity and classic aesthetics; the right side displays a biomimetic design that utilizes the natural textures and structures of sea urchins, highlighting a unique three-dimensionality and modern appeal. The rendering effect contrasts light and shadow variations along with material details, emphasizing the differences in aesthetics and functionality between the two designs, reflecting the influence of nature-inspired concepts on cultural and creative product design. Differentiated rendering effect as shown in **Figure 4**.

**Figure 5** presents a three-dimensional cross-sectional view of the biomimetic sea urchin-inspired porous structure, featuring a golden ratio spiral design and self-supporting cavities, exhibiting a uniform blue stress distribution. The semi-transparent heatmap gradient clearly illustrates the variation in stress values, with red areas indicating higher stress and blue areas showing lower stress. The peak stress of the traditional structure is 120 MPa, while the biomimetic structure significantly reduces to 65 MPa, highlighting the advantages and innovations of biomimetic design in mechanical performance. Mechanical structure rendering as shown in **Figure 5**.

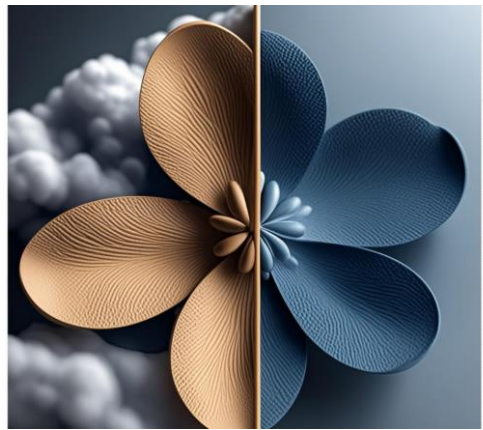


**Figure 4.** Differentiated rendering effect.

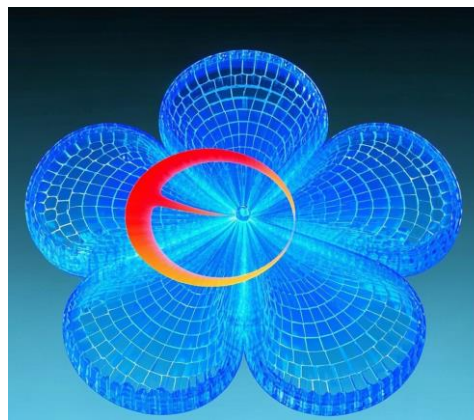


**Figure 5.** Mechanical structure rendering.

## 5. Conclusion

This paper explores the application of marine organism patterns in cultural and creative design from a biomechanical perspective, constructing a methodological system of “biomechanical decoding—pattern feature extraction—cultural and creative product transformation.” By modeling the quantitative relationship between marine organism morphological parameters and mechanical performance, it bridges the cognitive gap between bionic aesthetics and engineering mechanics. Taking the Dalian purple sea urchin as an example, it analyzes its unique radial structure and pentagonal internal arrangement, showcasing nature’s exquisite design in mechanical solutions. Through digital modeling and 3D printing technology to extract marine organism pattern elements, it is possible to create cultural and creative products that combine scientific and artistic qualities. Against the backdrop of rapid global development in the cultural and creative industry, the development and utilization of marine cultural symbols have become an important component of coastal countries’ cultural strategies. Applying biomechanical principles to cultural and creative design not only enhances product market competitiveness but also effectively inherits and promotes marine culture, showcasing the magical charm and unique value of marine organisms.

To achieve a deep integration of biomechanics and cultural design, a “dual track” interdisciplinary collaboration framework needs to be constructed, which harmonizes the paradigm differences between qualitative and quantitative methods through mixed

evaluation indicators. Firstly, establish an “Aesthetics Mechanics Collaborative Design Platform” that integrates cultural researchers’ morphological semantic analysis tools (such as Kansei evaluation in sensory engineering) with engineers’ quantitative verification systems (such as finite element simulation and fluid dynamics models) to form a closed-loop iterative process. Develop a mixed evaluation matrix to quantify subjective aesthetic elements (such as pattern rhythm and color coordination) into computable weight parameters (0–1 standardization), and perform multi-objective optimization with mechanical performance indicators (stress peak, drag reduction rate).

**Author contributions:** Conceptualization, RL and YX; methodology, RL; software, RL; validation, YX; formal analysis, YX; investigation, YX; resources, QH; data curation, QH; writing—original draft preparation, RL; writing—review and editing, RL; visualization, CZ; supervision, CZ project administration, YX; funding acquisition, RL and YX. All authors have read and agreed to the published version of the manuscript.

**Funding:** 1) This work was supported by the Anhui Provincial Quality Engineering Teaching Research Project for Higher Education Institutions: “Exploration and Practice of Transforming ‘Creative Market’ Club Activities into Aesthetic Education Courses” (Project Number: 2023jyxm0925). We extend our sincere gratitude for the support provided; 2) This work was supported by the project “Study on the Value of Intangible cultural Heritage in Dynamic Graphic Design -- Taking the 24 Solar Terms as an Example” (project approval number: 22YJA760089) of the Ministry of Education’s Humanities and Social Sciences Research Planning Fund in 2022; 3) This work was supported by the “Research on the Value of Intangible Cultural Heritage in Dynamic Graphic Design -- Taking the 24 Solar Terms as an Example” (Project number: DTR2023064), the Action Discipline (professional) leader cultivation project for young and middle-aged Teachers Training of Anhui Education Department of the CPC Anhui Provincial Committee in 2024 (Project number: DTR2023064); 4) This work has been supported by the Anhui Provincial University Research Project in 2023 (Anhui Provincial Research Planning Project), project category: Outstanding Youth research project “Anhui Provincial Opera Intangible cultural Heritage in Dynamic Graphic design Strategy Research” (project number: 2023AH030087), I would like to express my gratitude; 5) This work was supported by the Major Teaching Research Project of the Provincial Quality Engineering in Anhui Higher Education Institutions: “Innovation of Curriculum System for Cultural Heritage Research through Interdisciplinary Design Practice” (Project Number: 2022jyxm680). We express our gratitude for this support; 6) This work was supported by the Anhui Institute of Information Technology Youth Scientific Research Fund Project, “Research on the Design of Cultural and Creative Products for the Traditional Skills of Making Children’s Shoes and Hats in Hui Zhou Based on Meme Theory” (Project Number: 24QNJJSK005). We extend our sincere gratitude for the support provided.

**Ethical approval:** Not applicable.

**Informed consent statement:** Not applicable.

**Conflict of interest:** The authors declare no conflict of interest.

## References

1. Grafeld S, Oleson KLL, Teneva L, et al. Follow that fish: Uncovering the hidden blue economy in coral reef fisheries. *PLoS One*. 2017; 12(8): e0182104. doi: 10.1371/journal.pone.0182104
2. Ye S. Consumer experience and cultural and creative product design: The transition from functionality to emotion. *Green Packaging*. 2025; 2: 153–157.
3. Barthlott W, Mail M, Bhushan B, et al. Plant Surfaces: Structures and Functions for Biomimetic Innovations. *Nano-Micro Letters*. 2017; 9(2). doi: 10.1007/s40820-016-0125-1
4. Henrich J. Review of Bionics and Biomechanics Research. *Journal of Biomechanics*. 2022; 15(2): 123-135.
5. Korlević M. Pattern characteristics and fluid dynamics optimization of marine organisms. *Progress in Marine Science*. 2023; 32(4): 245-260.
6. Zhao Y. Research on the application of marine organism image elements in the design of Nixing ceramic cultural and creative products—Taking the “horseshoe crab” image as an example. *Ceramics*. 2024; 2: 77–80.
7. Zhang Z, Yan C, Han W, et al. Research on the application of marine organism images in blind box design. *Toy World*. 2024; 5: 178–180.
8. Bo Q, Jia L. Research on the application of morphological semantics in creative products of marine culture. *Design*. 2019; 32(16): 110–111.
9. Dacks R, Ticktin T, Jupiter SD, et al. Investigating the Role of Fish and Fishing in Sharing Networks to Build Resilience in Coral Reef Social-Ecological Systems. *Coastal Management*. 2020; 48(3): 165-187. doi: 10.1080/08920753.2020.1747911
10. Tian L. Research on the application of marine elements in ceramic cultural and creative design. *Tiangong*. 2024; 25: 60–62.
11. Delevaux JMS, Silver JM, Winder SG, et al. Social–ecological benefits of land–sea planning at multiple scales in Mesoamerica. *Nature Sustainability*. 2024; 7(5): 545-557. doi: 10.1038/s41893-024-01325-7
12. Liu Y. Research on the development path of creative design driven by artificial intelligence. *Screen Printing Industry*. 2025; 1: 67–69.
13. Yu Y. Research on innovative design strategies for marine cultural and creative products in Guangxi. *Tiangong*. 2024; 18: 60–62.
14. Delevaux JMS, Giardina CP, Kittinger JN. Scaling biocultural initiatives can support nature, food, and culture from summit to sea. *Sustainability*. 2020; 12(10): 4123.
15. Ding W, Zhang Q. Construction and design practice of cultural and creative IP design system based on design semiotics. *Art Grand View*. 2021; 3: 140–142.
16. Vaughan MB, Vitousek PM. Mahele: Sustaining Communities through Small-Scale Inshore Fishery Catch and Sharing Networks. *Pacific Science*. 2013; 67(3): 329-344. doi: 10.2984/67.3.3
17. Yu P. The application of marine cultural elements in the development and design of tourism products in Zhoushan. *Packaging Engineering*. 2019; 40(8): 305–310.
18. Zhang Y. Research on regional and personalized design of biomimetic cultural creative products for marine organisms. *Drama House*. 2019; 24: 127–128.
19. Vaughan MB, Kittinger JN. Mahele: Sustaining communities through small-scale inshore fishery catch and sharing networks. *Pacific Science*. 2016; 70(2): 234–250.
20. Ma K. Research on the design and cultural communication path of Haiyang cultural and creative products from the perspective of cultural identity. *Journal of Jilin Engineering and Technology Normal University*. 2022; 38(4): 45–47.
21. Zhang Y. Innovative design and research of biomimetic cultural creative products for marine organisms. *Art Education*. 2019; 6: 215–216.
22. Pascua P, McMillen H, Ticktin T, et al. Beyond services: A process and framework to incorporate cultural, genealogical, place-based, and indigenous relationships in ecosystem service assessments. *Ecosystem Services*. 2017; 26: 465-475. doi: 10.1016/j.ecoser.2017.03.012
23. Zhou Q, Zhao W. A review of research on generative artificial intelligence assisted text creation design methods. *Packaging Engineering*. 2025; 46(4): 121–133.
24. Winter KB, Beamer K, Vaughan MB, et al. The Moku System: Managing Biocultural Resources for Abundance within

- Social-Ecological Regions in Hawai'i. *Sustainability*. 2018; 10(10): 3554. doi: 10.3390/su10103554
25. Yang J. Creative research on ocean themed cultural and creative design—Taking carpets as an example. *Chemical Fiber and Textile Technology*. 2022; 51(3): 219–221.
  26. Ma W. Design cultural and creative products based on the protection of marine culture. *Western Leather*. 2021; 43(10): 105–106.